International Journal of Minerals, Metallurgy and Materials
Volume 22, Number 6, June 2015, Page 648
DOI: 10.1007/s12613-015-1118-7

High plastic Zr–Cu–Fe–Al–Nb bulk metallic glasses for biomedical applications

Shu-shen Wang, Yun-liang Wang, Yi-dong Wu, Tan Wang, and Xi-dong Hui

State Key Laboratory for Advanced Metals and Materials, University of Science and Technology Beijing, Beijing 100083, China
(Received: 14 October 2014; revised: 8 November 2014; accepted: 22 November 2014)

Abstract: Four Zr–Cu–Fe–Al-based bulk metallic glasses (BMGs) with Zr contents greater than 65at% and minor additions of Nb were designed and prepared. The glass forming abilities, thermal stabilities, mechanical properties, and corrosion resistance properties of the prepared BMGs were investigated. These BMGs exhibit moderate glass forming abilities along with superior fracture and yield strengths compared to previously reported Zr–Cu–Fe–Al BMGs. Specifically, the addition of Nb into this quaternary system remarkably increases the plastic strain to 27.5%, which is related to the high Poisson's ratio and low Young's and shear moduli. The Nb-bearing BMGs also exhibit a lower corrosion current density by about one order of magnitude and a wider passive region than 316L steel in phosphate buffer solution (PBS, pH 7.4). The combination of the optimized composition with high deformation ability, low Young's modulus, and excellent corrosion resistance properties indicates that this kind of BMG is promising for biomedical applications.

Keywords: metallic glasses; biomedical materials; mechanical properties; corrosion resistance; zirconium content; niobium addition

1. Introduction

Bulk metallic glasses (BMGs) are considered to be candidates for biomedical applications due to the atomic structure free from crystalline boundaries, superb strength, relatively low modulus, high corrosion resistance, and biocompatibility [1]. In the last decades, a series of Zr-based BMGs with the critical diameter ranging from the millimeter to the centimeter scale (e.g., Zr–Cu–Ni–Al [2–4], Zr–Cu–Ag–Al [5], Zr–Cu–Ni–Al–Ag [6–7], and Zr–Ti–Cu–Ni–Be [8–10]) have been developed. Most of these BMGs contain Ni and Be. Among the BMG components, Ni is known to be allergenic and possibly carcinogenic and should be avoided in long-term implantations. Accordingly, Ni-free Zr-based BMGs such as Zr–Cu–Fe–Al and Zr–Cu–Al–Co alloys have been developed for the biomedical purposes [11–12]. The $(Zr_xCu_{100-x})_{80}(Fe_{40}Al_{60})_{20}$ alloys with x = 68–77 show the excellent glass forming ability (GFA) [11]. $Zr_{60}Cu_{30-x}Fe_xAl_{10}$ (x = 0–10) alloys with the diameter larger than 10 mm have been synthesized by copper mold casting [12]. The compression strengths and plastic strains after yielding of these Zr–Cu–Fe–Al BMGs reach about 1700 MPa and 11.3%, respectively [13]. By replacing Fe with Co and Ag in Zr–Cu–Fe–Al BMGs, the compression yield stress can be further increased to about 2000 MPa [14].

To make this type of BMG more biocompatible and safe in human bodies, it is still necessary to optimize the compositions of Zr–Cu–Fe–Al BMGs. Although the reported Zr–Cu–Fe–Al BMGs are Ni-free, the Cu contents in previously reported Zr–Cu–Fe–Al BMGs have typically been high to obtain the large GFA. Biological reaction experiments have shown that Cu is also toxic to the human body after the Cu concentration surpasses the threshold value. Therefore, decreasing the content of Cu or, correspondingly, increasing the contents of Zr and Fe is beneficial to biomedical compatibility. The other issue of this kind of BMG for applications is the low fracture toughness. Due to the lack of a microstructure that can restrict the propagation of plastic flow bands, the fracture toughnesses of BMGs are generally lower than those of crystalline-structured metals. However, some BMGs with high-density shear bands are generated during the deformation process and do exhibit

Corresponding author: Xi-dong Hui E-mail: xdhui@ustb.edu.cn

high fracture toughnesses. The high fracture toughnesses of BMGs have been reported to be closely correlated to the high Poisson ratios (ν) of components [4]. As the Poisson ratios of Nb is up to 0.40, this element has been employed to strengthen Zr-based BMGs [15–16]. However, to date, no comprehensive study has been performed on Nb-containing Zr–Cu–Fe–Al BMGs, and an investigation of the strengthening mechanism of Nb in BMGs is particularly lacking. In this work, four Zr–Cu–Fe–Al-based BMGs were designed by increasing Zr content and reducing Cu content. A small amount of Nb was also added to enhance the potentials of these materials for biomedical applications. The GFAs and thermal stabilities of the four prepared alloys were characterized, and compressive tests were performed to reveal the influence of chemical composition on the strength and plasticity. Ultrasonic measurements were conducted to investigate the elastic moduli of these BMGs. The corrosion resistance properties were evaluated by electrochemical polarization curves. Finally, the potential of this kind of BMG for biomedical application was discussed.

2. Experimental

Four Zr-based BMGs with nominal compositions of $Zr_{66}Cu_{17.5}Fe_6Al_{10.5}$, $Zr_{67}Cu_{15}Fe_{7.5}Al_{10.5}$, $Zr_{70}Cu_{15.5}Fe_5Al_{9.5}$, and $Zr_{65.1}Cu_{17.2}Fe_{5.9}Al_{10.3}Nb_{1.5}$ (hereafter denoted as Z1, Z2, Z3, and Z4, respectively) were designed. The compositional features of these BMGs were the high content of Zr and relatively low content of Cu. Nb was further added into the quaternary Zr–Cu–Fe–Al alloys to achieve high plasticities.

The BMG alloy ingots were prepared by arc-melting Zr (99.9wt%), Cu (99.99wt%), Fe (99.9wt%), Al (99.9wt%), and Nb (99.9wt%) in a vacuum furnace under high-purity Ar atmosphere. The BMG rods with the diameter of ϕ2–5 mm and the length of 50 mm were prepared by water-cooling copper mold casting. The structures of samples were examined by using X-ray diffraction (XRD) with Cu K_α radiation (λ = 0.15406 nm). The thermal stability parameters associated with the glass transition (T_g) and crystallization temperature (T_x) were measured by differential scanning calorimetry (DSC; NETZSCH STA 449 C Jupiter) at heating rates ranging from 10 K/min to 40 K/min under Ar atmosphere. Uniaxial compressive tests were conducted at a strain rate of 2×10^{-4} s^{-1} in a CMT 4305 (China) instrument using the rods with the diameter of 2 mm and the length of 4 mm at room temperature. The fracture surface was examined by scanning electron microscopy (SEM; ZEISS Auriga). The elastic constants were obtained by an ultrasonic method (MATEC 6600 Ultrasound spectrometer) with an alloy specimen of ϕ3 mm × 6 mm. Electrochemical polarization was conducted in a three-electrode cell (Potentiostat/Galvanostat Model 273A) using a platinum counter electrode and a saturated calomel reference electrode (SCE). The entire cell was kept at 37°C throughout the test, and the electrolyte was phosphate buffer solution (PBS, pH 7.4) mixed with of 8 g/L NaCl, 0.2 g/L KCl, 1.14 g/L NaH_2PO_4, and 0.2 g/L KH_2PO_4 solutions.

3. Results and discussion

3.1. Glass forming ability and thermal stability

The relationship between the critical size and composition of BMG is one of the most important issues in the field of metallic glasses [1,17]. Fig. 1 shows the XRD patterns of the as-cast Z1–Z4 alloy rods with different diameters. All the XRD patterns exhibit a main halo peak, indicating the formation of the glassy structure in the specimens. The Z1 and Z4 alloys have the full glassy structure when the rods are 4 mm in diameter. Some crystal phases can be found in the Z1 and Z4 rods with the diameter of 5 mm. From the standard PDF cards, it can be seen that the crystalline phases in the Z1 and Z4 alloys are Al_2Zr_3 and $CuZr_2$, respectively. The critical diameters for the glass formation of the Z2 and Z3 alloys are lower than 4 mm, which are not shown in the XRD curves. Zhang *et al*. reported that $Zr_{60}Cu_{25}Fe_6Al_{10}$ and $Zr_{62.5}Cu_{22.5}Fe_6Al_{10}$ glassy alloys had the critical sizes above 10 mm [12]. In this work, it was shown that increasing Zr content indeed reduced the GFA. For the Z4 alloy, the addition of 1.5at% Nb did not reduce the GFA, but it changed the phase stabilities, resulting in the formation of $CuZr_2$.

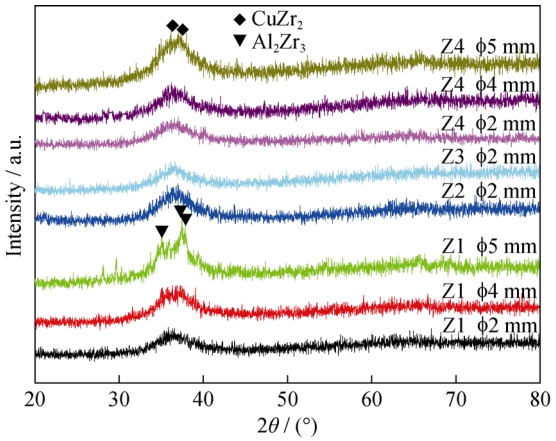

Fig. 1. X-ray diffraction patterns of Z1–Z4 alloy rods with different diameters.

The DSC curves of the as-cast Z1–Z4 glassy rods with the diameter of 2 mm are shown in Fig. 2(a), in which T_g

and T_x are marked with arrows. All the alloy samples exhibit a clear endothermic heat event caused by the glass transition followed by a crystallization process from the supercooled liquid to the equilibrium crystalline phases. The thermal stability parameters and critical diameters (D_c) of these BMGs determined from the DSC curves are summarized in Table 1. Notably, T_g and T_x increase from 639 K and 721 K for Z1 to 651 K and 745 K for Z4, respectively, leading to an increase in the supercooled liquid region ($\Delta T_x = T_x - T_g$) from 82 K for Z1 to 94 K for Z4. Namely, the addition of Nb increases the thermal stability of the alloy system. It is also seen that the liquidus temperature (T_l) of Z4 is the lowest among the four alloys. From these parameters, the criteria for the evaluation of GFA including ΔT_x, T_{rg}, γ, and α were calculated. As shown in Table 1, among the four BMGs, all these criteria are the highest for the Z4 alloy.

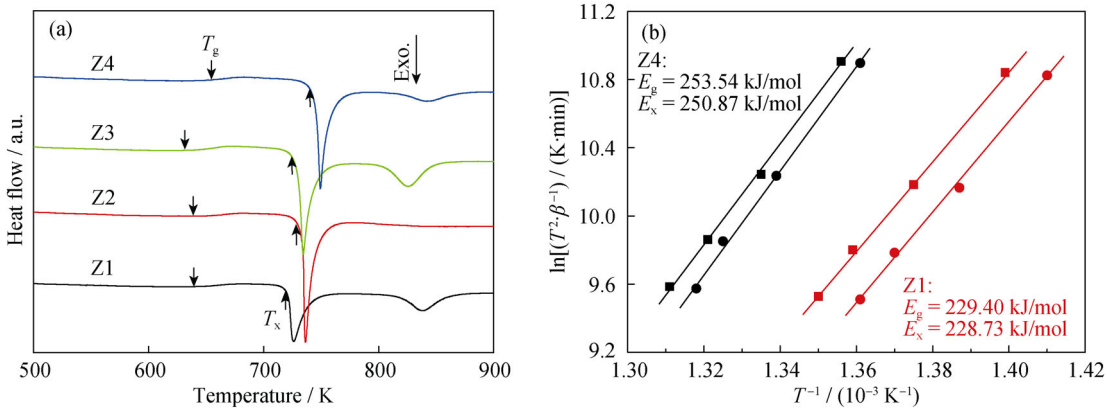

Fig. 2. (a) DSC curves of as-cast Z1–Z4 alloys rods with the diameter of 2 mm at 20 K/min; (b) Kissinger curves of ln(T^2/β) versus (1/T) for Z1 and Z4 metallic glasses.

Table 1. Thermal stability parameters and the criteria for evaluating the GFAs of Z1–Z4 BMGs

Alloy composition / at%	T_g / K	T_x / K	T_l / K	ΔT_x / K	T_{rg}	γ	α	D_c / mm
$Zr_{66}Cu_{17.5}Fe_6Al_{10.5}$ (Z1)	639	721	1145	82	0.558	0.404	0.630	4
$Zr_{67}Cu_{15}Fe_{7.5}Al_{10.5}$ (Z2)	638	731	1134	93	0.563	0.413	0.645	2
$Zr_{70}Cu_{15.5}Fe_5Al_{9.5}$ (Z3)	633	724	1131	91	0.560	0.410	0.640	2
$Zr_{65.1}Cu_{17.2}Fe_{5.9}Al_{10.3}Nb_{1.5}$ (Z4)	651	745	1128	94	0.577	0.419	0.660	4

Note: T_l is the liquidus temperature, $\Delta T_x = T_x - T_g$, $T_{rg} = T_g/T_l$, $\gamma = T_x/(T_g + T_l)$, and $\alpha = T_x/T_l$.

The effect of Nb addition on the thermal stabilities of Zr–Cu–Fe–Al alloys can be also evaluated by comparing the activation energies of Z1 and Z4 BMGs. For this purpose, the Z1 and Z4 alloys were analyzed with DSC at heating rates of 10, 20, 30, and 40 K/min, and the T_g and T_x under different heating rates were obtained from the DSC curves. Based on these characteristic temperatures, the activation energies were studied using the Kissinger equation [18], which is expressed as

$$\ln\left(\frac{\beta}{T^2}\right) = -\frac{E}{RT} + A \quad (1)$$

where β is the heating rate (K/min), T the temperature that represents T_g or T_x (K), R the gas constant (8.314 J·mol^{-1}·K^{-1}), E the activation energy, and A a constant. The relational graphs of ln(T^2·β^{-1}) vs. T^{-1} for Z1 and Z4 alloys are shown in Fig. 2(b), where E_g and E_x stand for the activation energies of glass transition and crystallization, respectively. The activation energy is known to indicate the potential barrier for a phase transformation; the thermal stability will be increased if the activation energy is increased. From Fig. 2(b), E_g and E_x are calculated to be 229.40 and 228.73 kJ/mol for Z1 and 253.54 and 250.87 kJ/mol for Z4, respectively. Both the E_g and E_x values of the Z4 alloy are higher than those of Z1. Thus, it can be deduced that the thermal stability of Zr–Cu–Fe–Al alloys is obviously increased by the addition of Nb.

3.2. Mechanical properties

To evaluate the mechanical properties of the four BMGs, room-temperature compression tests were performed for the BMG rods with the diameter of 2 mm. Fig. 3 shows the engineering stress-strain curves of the BMGs at a compression strain rate of 2×10^{-4} s^{-1}. The mechanical properties of the present BMGs and previously reported Zr–Cu–Fe–Al-based

glassy alloys are listed in Table 2 [13,19–20], including the compressive fracture strength (σ_f), yield strength (σ_y), and plastic strain (ε_p). All the glassy alloys except Z1 exhibit the superior fracture strength or yield strength compared to previously reported BMGs. Particularly, the plastic strain of the Z4 BMG reaches 27.5%, which is larger than those of Z1 and $Zr_{60}Cu_{20}Fe_5Al_{10}Nb_5$ [19] by 235.4% and 141.2%, respectively. Therefore, minor additions of Nb are considered to significantly enhance the mechanical properties of Zr–Cu–Fe–Al metallic glasses.

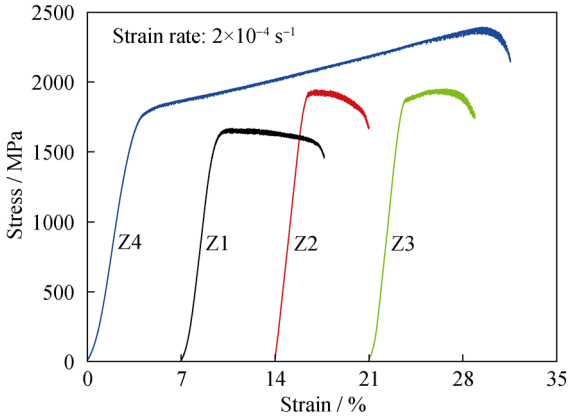

Fig. 3. Compressive stress-strain curves of Z1–Z4 glassy rods with the diameter of 2 mm.

Fig. 4 shows the SEM images of the lateral surfaces of Z1 and Z4 BMGs alloys after compression fracturing. Both of the alloy rods show the typical shear fracture features of conventional BMGs. The fracture surfaces of Z1 and Z4 BMGs present angles of 44.1° and 43.3°, respectively, with respect to the stress axis, as shown in Figs. 4(a) and (c). It is noticed that the Z4 sample forms a "drum" shape after compression, indicating that it has experienced enhanced plastic deformation. A large amount of shear bands presents on the specimen surface, as shown in Figs. 4(b) and (d). In addition to the primary shear bands (marked by white arrows), there are also secondary shear bands (marked by red arrows). The secondary shear bands in Z4 alloy are denser than those in Z1 alloy, indicating that the severe shear deformation takes place by the initiation and propagation of shear bands.

Table 2. Mechanical properties of the BMGs produced in this study along with previously reported Zr–Cu–Fe–Al BMGs

Alloy composition / at%	σ_f / MPa	σ_y / MPa	ε_p / %	Strain rate / s^{-1}
$Zr_{66}Cu_{17.5}Fe_6Al_{10.5}$ (Z1)	1666	1527	8.2	2×10^{-4}
$Zr_{67}Cu_{15}Fe_{7.5}Al_{10.5}$ (Z2)	1941	1887	4.9	2×10^{-4}
$Zr_{70}Cu_{15.5}Fe_5Al_{9.5}$ (Z3)	1947	1840	5.4	2×10^{-4}
$Zr_{65.1}Cu_{17.2}Fe_{5.9}Al_{10.3}Nb_{1.5}$ (Z4)	2391	1655	27.5	2×10^{-4}
$Zr_{60}Cu_{20}Fe_5Al_{10}Nb_5$ [19]	1795	1393	11.4	1×10^{-4}
$Zr_{60}Cu_{22.5}Fe_{7.5}Al_{10}$ [13]	1718	—	9.2	5×10^{-4}
$Zr_{60}Cu_{20}Fe_{10}Al_{10}$ [13]	1708	—	9.5	5×10^{-4}
$Zr_{60}Cu_{17.5}Fe_{12.5}Al_{10}$ [13]	1725	—	11.3	5×10^{-4}
$Zr_{60}Cu_{25}Fe_5Al_{10}$ [20]	—	1643	4.4	5×10^{-4}
$Zr_{62.5}Cu_{22.5}Fe_5Al_{10}$ [20]	—	1548	5.1	5×10^{-4}
$Zr_{65}Cu_{20}Fe_5Al_{10}$ [20]	—	1594	5.2	5×10^{-4}
$Zr_{67.5}Cu_{17.5}Fe_5Al_{10}$ [20]	—	1498	3.7	5×10^{-4}

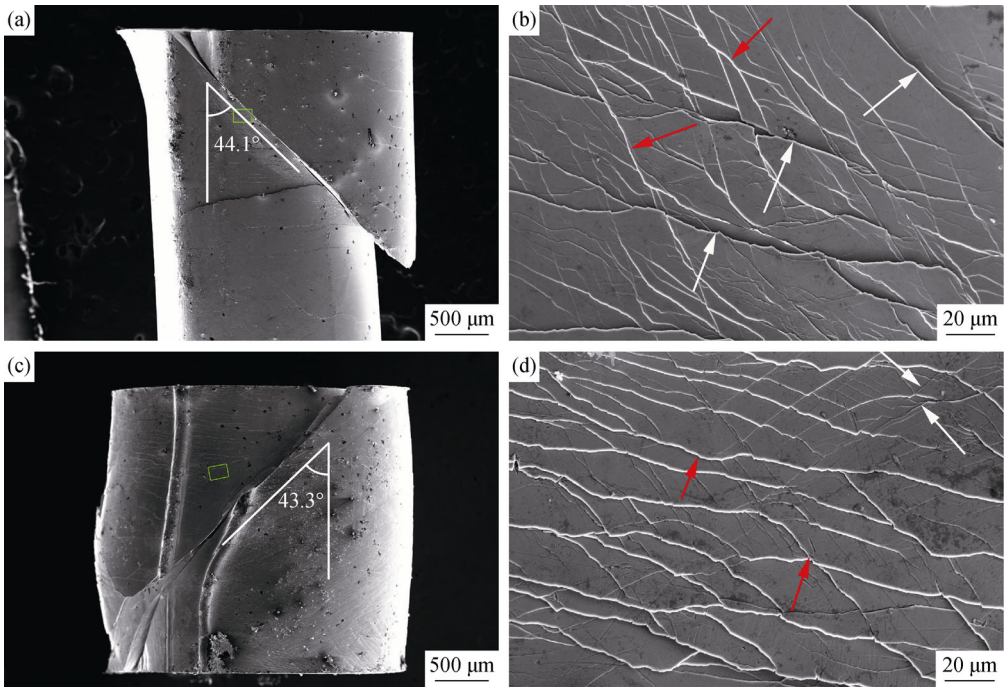

Fig. 4. SEM images of the lateral surfaces of Z1 ((a) and (b)) and Z4 alloy ((c) and (d)) rods after compression deformation.

The excellent deformation abilities of these BMGs are probably related to the large Poisson ratios (v), which satisfy Eq. (2) [21].

$$G = \frac{E}{2(1+v)} \tag{2}$$

where G is the shear modulus, and E is the Young's modulus. The E, G, and v values are 76.8 GPa, 27.9 GPa, and 0.375 for Z1, and 73.2 GPa, 26.4 GPa, and 0.384 for Z4, respectively. The low Young's modulus is very important for applying these types of BMGs as biomedical materials. It is seen that the E and G values of Z4 alloy are lower than those of Z1, whereas the v value of Z4 alloy is higher than that of Z1. The decrease in G and increase in v are beneficial to the plastic deformation of BMGs. The lower G means that the shear bands are more easily initiated [21–22]; thus, a high density of shear bands can be easily formed under compressive loading, resulting in the increased resistance to plastic strain. The results of Poisson ratios are in good agreement with those indicated by the compressive curves and shear bands on the lateral surfaces of the BMGs.

3.3. Corrosion resistance properties

The polarization curves of Z4 BMG and 316L stainless steel in PBS are shown in Fig. 5. The corrosion properties associated with the free corrosion potential (E_{corr}), corrosion current density (i_{corr}), and passivation current density (i_p) are listed in Table 3. E_{corr} is an inherent property of a given material and may be employed to characterize the corrosion resistance property of an alloy. The values of E_{corr} and i_{corr} are –0.42 V and 3.48 μA·cm^{-2} for Z4, and –0.25 V and 36.3 μA·cm^{-2} for 316L steel, respectively. The i_p of the Z4 glassy alloy and 316L steel are almost the same. The curve of the Z4 glassy alloy shows a wider passive region than that of 316L steel. The results demonstrate that 316L steel has a

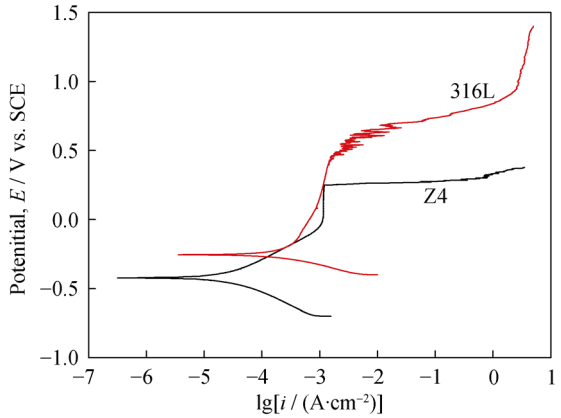

Fig. 5. Polarization curves of Z4 BMG and 316L stainless steel in PBS.

Table 3. Corrosion properties of Z4 BMG and 316L stainless steel

Alloys	E_{corr} / V	i_{corr} / (μA·cm^{-2})	i_p / (μA·cm^{-2})
$Zr_{65.1}Cu_{17.2}Fe_{5.9}Al_{10.3}Nb_{1.5}$ (Z4)	−0.42	3.48	2.15
316L steel	−0.25	36.3	2.19

higher E_{corr} than Z4 due to its high Cr content (16wt%–18wt%). The i_{corr} of Z4 BMG is lower than that of 316L steel by almost one order, indicating that the corrosion rate of the Z4 alloy is very low in PBS. Their excellent corrosion resistance properties in PBS indicate that this kind of BMG has a good potential for biomedical applications.

4. Conclusions

(1) The four Zr–Cu–Fe–Al alloys prepared in this work show fine GFAs and thermal stabilities. The addition of Nb increases the thermal stability of this kind of BMG, as characterized by the higher glass transition and crystallization temperatures, wider supercooled liquid regions, and larger glass transition and crystallization activation energies of the Nb-bearing BMGs.

(2) The glassy alloys prepared in this work exhibit superior fracture strengths or yield strengths compared to previously reported BMGs. In particular, Z4 BMG shows an excellent deformation ability with a plastic strain of 27.5%. In addition to the primary shear bands, secondary shear bands are also observed on the lateral surfaces of these BMGs. The secondary shear bands in the Z4 alloy are denser than those in the Z1 alloy.

(3) The Z4 BMG alloy has a higher Poisson ratio and a lower Young's modulus and shear modulus than the Z1 alloy, which are beneficial to the shear deformation of BMGs. The low Young's modulus is beneficial for the application of the BMGs as biomedical materials.

(4) The Z4 BMG alloy exhibits a lower corrosion current density by about one order and shows a wider passive region than 316L steel in PBS, indicating that this kind of BMG exhibits the excellent corrosion resistance properties.

Acknowledgements

This work was financially supported by the National Natural Science Foundation of China (No. 51271018) and the Proprietary Program of the State Key Laboratory for Advanced Metals and Materials, University of Science and Technology Beijing (Nos. 2011Z-01 and 2012Z-01).

References

[1] A. Inoue, Stabilization of metallic supercooled liquid and bulk amorphous alloys, *Acta Mater.*, 48(2000), No. 1, p. 279.

[2] Y. Yokoyama, K. Fukaura, and A. Inoue, Cast structure and mechanical properties of Zr–Cu–Ni–Al bulk glassy alloys, *Intermetallics,* 10(2002), No. 11-12, p. 1113.

[3] Q.S. Zhang, W. Zhang, X.M. Wang, Y. Yokoyama, K. Yubuta, and A. Inoue, Structure, thermal stability and mechanical properties of $Zr_{65}Al_{7.5}Ni_{10}Cu_{17.5}$ glassy alloy rod with a diameter of 16 mm produced by tilt casting, *Mater. Trans.*, 49(2008), No. 9, p. 2141.

[4] A. Inoue, T. Shibata, and T. Zhang, Effect of additional elements on glass transition behavior and glass formation tendency of Zr–Al–Cu–Ni alloys, *Mater. Trans. JIM*, 36(1995), No. 12, p. 1420.

[5] G.Q. Zhang, Q.K. Jiang, L.Y. Chen, M. Shao, J.F. Liu, and J.Z. Jiang, Synthesis of centimeter-size Ag-doped Zr–Cu–Al metallic glasses with large plasticity, *J. Alloys Compd.*, 424(2006), No. 1-2, p. 176.

[6] A. Inoue, T. Zhang, M.W. Chen, and T. Sakurai, Mechanical properties of bulk amorphous Zr–Al–Cu–Ni–Ag alloys containing nanoscale quasicrystalline particles, *Mater. Trans. JIM*, 40(1999), No. 12, p. 1382.

[7] J.K. Lee, G. Choi, D.H. Kim, and W.T. Kim, Formation of icosahedral phase from amorphous $Zr_{65}Al_{7.5}Cu_{12.5}Ni_{10}Ag_5$ alloys, *Appl. Phys. Lett.*, 77(2000), No. 7, p. 978.

[8] W.L. Johnson, Bulk glass-forming metallic alloys: science and technology, *MRS Bull.*, 24(1999), No. 10, p. 42.

[9] T.A. Waniuk, J. Schroers, and W.L. Johnson, Critical cooling rate and thermal stability of Zr–Ti–Cu–Ni–Be alloys, *Appl. Phys. Lett.*, 78(2001), No. 9, p. 1213.

[10] B.Y. Zhang, X.H. Chen and X. D. Hui, A coating thickness controlling model in continuously fabricating metallic glass-coated composite wires, *Int. J. Miner. Metall. Mater.*, 20(2013), No. 5, p. 456.

[11] K.F. Jin and J.F. Löffler, Bulk metallic glass formation in Zr–Cu–Fe–Al alloys, *Appl. Phys. Lett.*, 86(2005), No. 24, p. 241909.

[12] Q.S. Zhang, W. Zhang, and A. Inoue, Ni-free Zr–Fe–Al–Cu bulk metallic glasses with high glass-forming ability, *Scripta Mater.*, 61(2009), No. 3, p. 241.

[13] Q.S. Zhang, W. Zhang, D.V. Louuzguine, and A. Inoue, High glass-forming ability and unusual deformation behavior of new Zr–Cu–Fe–Al bulk metallic glasses, *Mater. Sci. Forum*, 654-656(2010), p. 1042.

[14] K. Mondal, T. Ohkubo, T. Mukai, and K. Hono, Glass forming ability and mechanical properties of quinary Zr-based bulk metallic glasses, *Mater. Trans.*, 48(2007), No. 6, p. 1322.

[15] G.W.C. Kaye and T.H. Laby, *Tables of Physical and Chemical Constants*, Longman, London, 1921.

[16] X.H. Chen, B.Y. Zhang, and X.D. Hui, Effect of Nb on the corrosion behavior of continuous bulk metallic glass-coated steel wire composites. *Int. J. Miner. Metall. Mater.*, 20(2013), No. 6, p. 589.

[17] A. Inoue and A. Takeuchi, Recent development and application products of bulk glassy alloys, *Acta Mater.*, 59(2011), No. 6, p. 2243.

[18] H.E. Kissinger, Reaction kinetics in differential thermal analysis, *Anal. Chem.*, 29(1957), No. 11, p. 1702.

[19] L. Liu, C.L. Qiu, Q. Chen, K.C. Chan, and S.M. Zhang, Deformation behavior, corrosion resistance, and cytotoxicity of Ni-free Zr-based bulk metallic glasses, *J. Biomed. Mater. Res. A*, 86A(2007), No. 1, p. 160.

[20] Q.S. Zhang, W. Zhang, G.Q. Xie, D.V. Louzguine-Luzgin, and A. Inoue, Stable flowing of localized shear bands in soft bulk metallic glasses, *Acta Mater.*, 58(2010), No. 3, p. 904.

[21] Y. Yokoyama, K. Fujita, A.R. Yavari, and A. Inoue, Malleable hypoeutectic Zr–Ni–Cu–Al bulk glassy alloys with tensile plastic elongation at room temperature, *Philos. Mag. Lett.*, 89(2009), No. 5, p. 322.

[22] N.B. Hua, S.J. Pang, Y. Li, J.F. Wang, R. Li, K. Georgarakis, A.R. Yavari, G. Vaughan, and T. Zhang, Ni- and Cu-free Zr–Al–Co–Ag bulk metallic glasses with superior glass-forming ability, *J. Mater. Res.*, 26(2011), No. 4, p. 539.